

All-electrical measurement of the triplet-singlet spin relaxation time in self-assembled quantum dots

K. Eltrudis,^{1,a)} A. Al-Ashouri,¹ A. Beckel,¹ A. Ludwig,² A. D. Wieck,² M. Geller,¹ and A. Lorke^{1,b)}

¹Faculty of Physics and CENIDE, University of Duisburg-Essen, Lotharstr. 1, 47057 Duisburg, Germany

²Chair for Applied Solid State Physics, Ruhr-Universität Bochum, Universitätsstr. 150, 44780 Bochum, Germany

(Received 31 May 2017; accepted 15 August 2017; published online 29 August 2017)

We have measured the spin relaxation time of an excited two-electron spin-triplet state into its singlet ground state in self-assembled InAs/GaAs quantum dots. We use a time-resolved measurement scheme that combines transconductance spectroscopy with spin-to-charge conversion to address the $|s \uparrow, p \uparrow\rangle$ triplet state, where one electron is in the quantum dot s -shell and a second one in the p -shell. The evaluation of the state-selective tunneling times from the dots into a nearby two-dimensional electron gas allows us to determine the s - and p -shell occupation and extract the relaxation time from a rate equation model. A comparably long triplet-to-singlet spin relaxation time of $25 \mu\text{s}$ is found. Published by AIP Publishing. [<http://dx.doi.org/10.1063/1.4985572>]

The spin dynamics in semiconductor quantum dots¹ has attracted much attention, as it is of fundamental interest for applications in quantum information processing.² The electron spin as an ideal two-level system may be used as a quantum bit (Qubit), for instance, in quantum computation³ or quantum memories.⁴ Quantum computation requires long coherence times, where the main obstacle for spin-based quantum information processing is the spin relaxation T_1 - and the spin dephasing T_2 -time, i.e., the longitudinal and transverse spin decay time, respectively.^{1,5,6} Even today, after years of extensive research, it remains an important challenge to understand in detail the spin relaxation mechanisms⁷ and find experimental methods to increase the spin relaxation and dephasing time. Especially, a spin state configuration with large spin relaxation times in the zero magnetic field and at moderately low temperatures would be advantageous for future applications in quantum information processing.

Here, we present an all-electrical measurement to prepare and monitor an excited spin-triplet state with a large energy mismatch to the ground ($\sim 50 \text{ meV}$) and excited ($\sim 10 \text{ meV}$) spin singlet states. We follow a measurement scheme of spin-to-charge conversion that was developed in lithographically defined nanostructures^{8,9} and combine it with transconductance spectroscopy, suitable for studying the carrier dynamics in self-assembled quantum dots.^{10–14} A time $T_1 = 25 \mu\text{s}$ is found for the spin relaxation from the triplet state $|s \uparrow, p \uparrow\rangle$ down to the singlet ground state $|s \uparrow, s \downarrow\rangle$.

The sample was fabricated using molecular beam epitaxy as an inverted high electron mobility transistor (HEMT) with an embedded layer of InAs quantum dots. The heterostructure was grown on a semi-insulating GaAs(001) substrate, starting with 150 nm of $\text{Al}_{0.34}\text{Ga}_{0.66}\text{As}$ and a 100 nm thick digital alloy ($33 \times [2 \text{ nm GaAs} + 1 \text{ nm AlAs}] + 1 \text{ nm GaAs}$), followed by a silicon δ -doping, 23 nm of digital alloy, and a

$19 \text{ nm Al}_{0.34}\text{Ga}_{0.66}\text{As}$ spacer layer. A two-dimensional electron gas (2DEG) is formed at the interface between the (AlGa)As layers and a 40 nm thick layer of GaAs [see Fig. 1(a)]. The InAs quantum dots were grown by deposition of about 1 monolayer of InAs. They were covered by 30 nm GaAs, a superlattice, ($50 \times [3 \text{ nm AlAs} + 1 \text{ nm GaAs}]$), and a 10 nm thick GaAs capping layer. The device was patterned into a transistor structure with source, drain, and gate contacts [cf. Fig. 1(b)], using standard optical lithography methods. The active region, formed by a 100 nm thick gold electrode, has a length of $100 \mu\text{m}$ and a width of $20 \mu\text{m}$, corresponding to about 2×10^5 dots that are simultaneously probed. The source and drain contacts were realized by evaporation of Ni, AuGe, and Au and subsequent thermal annealing. All measurements were carried out at a temperature of 4 K in a helium-free cryostat.

The measurement technique is based on the time-resolved transconductance spectroscopy,^{11,13} which was recently employed to selectively populate spin singlet and triplet states.^{10,13} A small, constant source-drain voltage $V_{SD} = 20 \text{ mV}$ is applied, and the conductance of the 2DEG, $G_{SD} = I_{SD}/V_{SD}$ is determined by measuring the source drain current I_{SD} . The time resolution is given by the RC time constant of the sample of $1 \mu\text{s}$. When a positive voltage pulse V_p is applied to the gate [see Fig. 1(b)], G_{SD} will first abruptly increase as a result of the increased carrier density in the 2DEG. The voltage pulse will also lower the energy of the quantum dot states, so that electrons can tunnel from the 2DEG to the quantum dot layer. This will decrease again the carrier density in the 2DEG, so that a decrease in G_{SD} is observed on a time scale of a few $10 \mu\text{s}$, characteristic for the tunneling time between the 2DEG and the quantum dots [Fig. 1(c)].

The derivative dG_{SD}/dV_p reflects the time-dependent density of states (DOS) in the dot layer¹³ and makes it possible to monitor the complete time evolution as the dots are filling up with electrons.¹¹ Figure 2(a) shows a snapshot of dG_{SD}/dV_p at a time $t_c = 5.8 \mu\text{s}$. Here, the initial gate voltage

^{a)}Electronic mail: kevin.eltrudis@uni-due.de

^{b)}Electronic mail: axel.lorke@uni-due.de

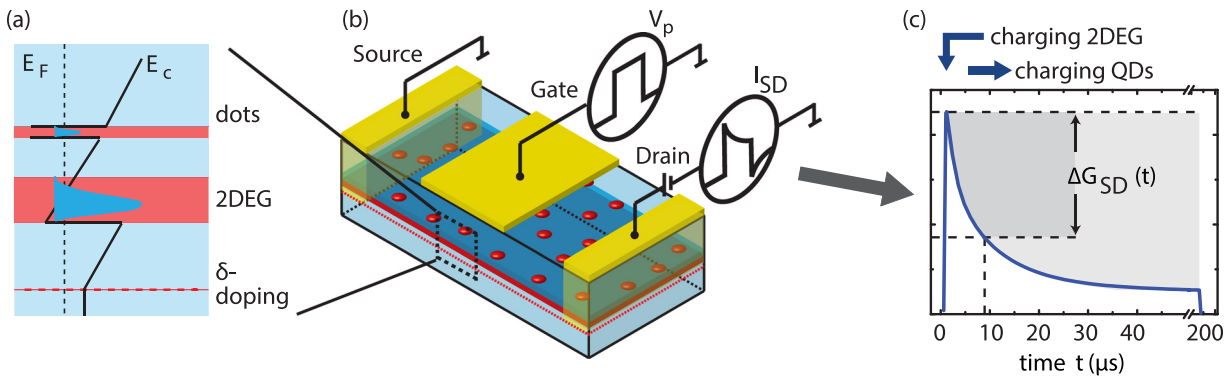


FIG. 1. (a) and (b) Schematic representation of the sample structure with the two dimensional electron gas (2DEG, red layer) and the quantum dots (red) embedded in an (AlGa)As field-effect structure. A small constant voltage is applied to the source and drain contacts, and the time-resolved change in current ΔI_{SD} is recorded when a voltage pulse V_p is applied to the top gate (b). Thus, the determined change in conductance ΔG_{SD} (c) is directly given by the tunneling of electrons from the extended 2DEG to the localized dot states, where they no longer contribute to the conductivity.

$V_i = -0.53$ V is chosen so that the initial charge in the quantum dot layer is ≈ 1 electron per dot, and the two-electron DOS is probed by increasing the pulse height V_p .¹³ In Fig. 2(a), three main features can be observed. They can be identified based on previous experiments and calculations^{11,13} as shown in the schematic insets: The charging of the second electron into the lowest state (*s*-state) takes place at $V_p = 0.04$ V. The occupation of the first excited state (*p*-state) is observed around $V_p = 0.36$ V. The maximum at $V_p = 0.6$ V corresponds to the charging of the *d*-state. A double peak structure of the *p*-state filling is observed, indicating the selective population of the triplet state at $V_p = 0.32$ V and the singlet state at $V_p = 0.41$ V.^{11,13}

We use the different relaxation properties of the singlet and triplet states and distinguish them by the time dependence of their *discharging* characteristics. The relaxation from the excited singlet state $|s \uparrow, p \downarrow\rangle$ to the ground state $|s \uparrow, s \downarrow\rangle$ is dipole-allowed and will take place in the range of nanoseconds. Tunneling out of the ground state will be slow because of the higher effective tunneling barrier.¹⁵ The energy relaxation of the triplet state $|s \uparrow, p \uparrow\rangle \rightarrow |s \uparrow, s \downarrow\rangle$, on the other hand, requires a spin flip and will therefore be much slower. During the relaxation time, tunneling out of the dots from the *p*-level will be possible, which is much faster than tunneling out of the *s*-state.

Therefore, for electrons injected into the *p*-shell, two different time constants are observed in the discharging

characteristics [see Fig. 2(b)]. From a double exponential fit to the data, we determine the characteristic time and amplitude for tunneling out of the *p*-state (fast) and the *s*-state (slow). Figure 2(c) summarizes the amplitudes of the fast and slow contributions for all pulse heights as blue and red lines, respectively. The fact that the slow contribution is at lower energy and that the spacing of both lines (≈ 13 meV)^{16,18,19} agrees with the exchange interaction in similar self-organized quantum dots,¹¹ confirms the assignment in Fig. 2(c) of the triplet and singlet states. In essence, the separation into a slow and a fast tunneling contribution to individually detect the triplet and singlet states corresponds to the “spin-to-charge conversion” techniques that have been developed for lithographically defined quantum dots.⁹

This now enables us, in an all-electric measuring scheme, to determine the triplet spin relaxation time in self-organized InAs quantum dots. We set V_p to 0.33 V, so that electrons will be injected into the triplet state. By increasing the charging time, i.e., the duration of the charging pulse, we allow the electrons to (partially) undergo a spin-flip and relax down to the *s*-shell. Then, we analyze the discharging signal as described above and determine the fraction of electrons that are in the excited state. The data points in Fig. 3(a) show the amplitudes of the fast (A_{fast} , blue) and the slow (A_{slow} , red) contributions as a function of the charging time t_c . It can be observed that for short t_c , the fast contribution dominates. The rise time of A_{fast} of about 10 μ s reflects the tunneling

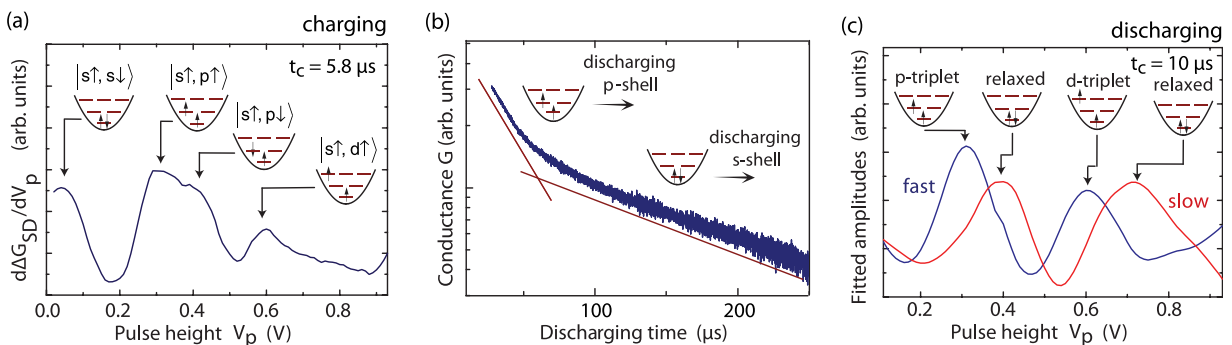


FIG. 2. (a) Charging spectrum for the injection of a second electron into the dots. The pictograms illustrate (from left to right) the injection of the second electron into the singlet ground state, the two-electron triplet state, the excited singlet state, and the *d*-shell, respectively. (b) Semilogarithmic plot of the discharging transient, showing the double-exponential behavior, originating from tunneling out of the *s*- and the *p*-shell. (c) Discharging amplitudes for the slow (red) and fast (blue) contribution in (b) as a function of the pulse height V_p . Note the separation of the double peak in (a) into a fast tunneling triplet and a slow tunneling singlet state.

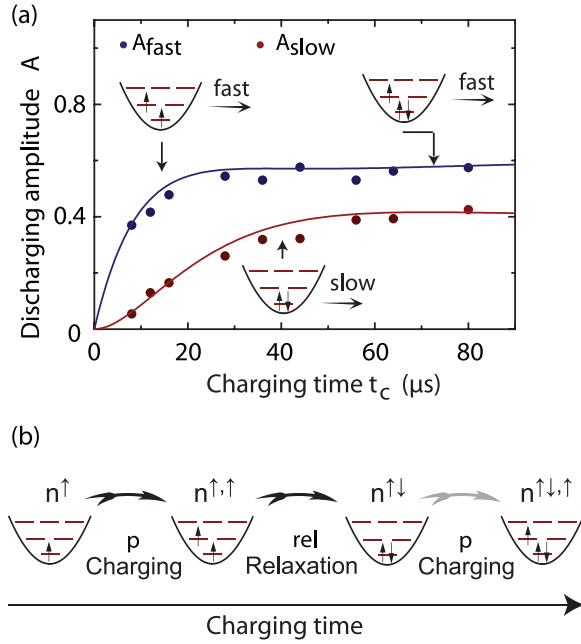


FIG. 3. (a) Emission amplitudes as a function of the charging time (data points). The solid lines are the results of a fit, based on a simple relaxation model. (b) Schematic of the different charging and relaxation steps that are considered in the model. The last step (tunneling of a third electron) is only possible for a fraction λ of the dots.

time of electrons from the 2DEG into the p -shell of the dots, where they form the triplet state. At longer charging times, also the slow contribution increases in amplitude, as more and more electrons relax down to the ground state. The corresponding depletion of the triplet state should lead to a decrease in the fast contribution. However, we find an almost constant A_{fast} for times $t_c > 20 \mu\text{s}$. The reason for this behavior is the fact that a third electron can tunnel into the dot after the relaxation of the triplet state [see Fig. 3(b), right]. The third electron cannot relax into the (already filled) s -shell and will therefore remain in the p -state and lead to a fast discharging signal, independent of the waiting time. In principle, the 3-electron state has a higher energy than the 2-electron triplet state;¹¹ however, because of the inhomogeneous broadening of the dot ensemble, a fraction λ of the dots will allow tunneling into the 3-electron ground state.¹³

To more quantitatively model the time evolution of the emission amplitudes in Fig. 3(a), we use a system of rate equations, following the sequence of events depicted in Fig. 3(b)

$$\frac{dn^\uparrow}{dt} = -\frac{n^\uparrow}{\tau_p}, \quad (1)$$

$$\frac{dn^{\uparrow,\uparrow}}{dt} = \frac{n^\uparrow}{\tau_p} - \frac{n^{\uparrow,\uparrow}}{\tau_{rel}}, \quad (2)$$

$$\frac{dn^{\uparrow\downarrow}}{dt} = \frac{n^{\uparrow,\uparrow}}{\tau_{rel}} - \left[\frac{n^{\uparrow\downarrow}}{\tau_p} \right], \quad (3)$$

$$\frac{dn^{\uparrow\downarrow,\uparrow}}{dt} = \frac{n^{\uparrow\downarrow}}{\tau_p}. \quad (4)$$

Here, τ_p is the characteristic time for electron tunneling into the p -state, and τ_{rel} is the spin relaxation time. The

number of dots in the states $|s^\uparrow\rangle$, $|s^\uparrow, p^\uparrow\rangle$, $|s^\uparrow, s^\downarrow\rangle$ and $|s^\uparrow, s^\downarrow, p^\uparrow\rangle$ are labelled n^\uparrow , $n^{\uparrow,\uparrow}$, $n^{\uparrow\downarrow}$ and $n^{\uparrow\downarrow,\uparrow}$, respectively [see also Fig. 3(b)]. The amplitudes of the slow and the fast emission signals are then determined from $n^{\uparrow\downarrow}$ and $n^{\uparrow,\uparrow} + n^{\uparrow\downarrow,\uparrow}$, respectively. Note that the tunneling into the $n^{\uparrow\downarrow,\uparrow}$ -state [Eq. (4) and term in brackets in Eq. (3)] will only be considered for a fraction λ of the dots, as discussed earlier.

The calculated normalized emission amplitudes as a function of the charging time are shown as solid lines in Fig. 3(a) for $\tau_p = 14 \pm 2 \mu\text{s}$,¹⁷ $\tau_{rel} = 25 \mu\text{s}$, and $\lambda = 0.6$. For these parameters, we find good agreement between the experimental data and the model for both the fast and the slow discharging signals. This allows us to determine the triplet spin relaxation time, τ_{rel} , of $25 \pm 5 \mu\text{s}$ in self-organized InAs quantum dots. The margin of error was estimated from a systematic variation of τ_{rel} and a comparison with the experimental data.

Our results add an important piece of information to the active field of spin relaxation in quantum dots, a mechanism which is of great interest for applications in quantum information technologies. Spin relaxation times in quantum dots have been extensively studied,^{9,20–23,28–31} however, mostly in a regime where the spin-flip was accompanied by only a small energy relaxation (e.g., spin-flip within the s -shell).^{7,24} In this regime, spin relaxation times up to 20 ms were found.⁷ The triplet-singlet transition with energy relaxation from the p -shell to the s -shell was studied, for instance, by Fujisawa *et al.*²⁵ and Hanson *et al.*⁹ in lithographically defined dots. They found a relaxation time of $200 \mu\text{s}$ and 2.58 ms for an energy difference ΔE_{p-s} of $2.5\text{--}5.5 \text{ meV}$ and ΔE_{p-s} smaller than 1 meV , respectively. In the present dots, $\Delta E_{p-s} = 50 \text{ meV}$,¹¹ a value that is higher than the optical phonon energies of the (InGa)As system.²⁶ Therefore, a very efficient, polariton-mediated spin relaxation is expected, which— together with the 10–100 times higher temperature—can explain the considerably shorter lifetime in the present experiment. Theoretical estimates of the phonon-assisted spin-flip transition between the first excited and the ground state range from 10^2 s to 10^{-5} s for parameters that are more appropriate for lithographically defined quantum dots.²⁷ We hope that our data will provide a reference point for future theoretical treatments of spin relaxation in semiconductor nanostructures.

Finally, we would like to point out that the relatively long spin relaxation time in the present experiment was achieved without the application of an external magnetic field and at moderately low temperatures, which are easily achieved in low maintenance, helium-free cryostats.

In summary, we have combined time-resolved transconductance spectroscopy with a spin-to-charge-conversion technique to obtain the two-electron, triplet-to-singlet spin relaxation time in self-assembled InAs quantum dots. We find a comparably long relaxation time $\tau_{rel} = 25 \mu\text{s}$ at liquid helium temperatures and without the need to apply an external magnetic field.

This work was supported by the German Research Foundation under Grant No. SFB 1242, TP A01. The authors would like to thank Peter Kratzer and Annika Kurzmann for valuable discussions.

- ¹R. Hanson, L. P. Kouwenhoven, J. R. Petta, S. Tarucha, and L. M. K. Vandersypen, *Rev. Mod. Phys.* **79**, 1217 (2007).
- ²S. Benjamin, B. Lovett, and J. Smith, *Laser Photon. Rev.* **3**, 556 (2009).
- ³C. H. Bennett and D. P. DiVincenzo, *Nature* **404**, 247 (2000).
- ⁴R. J. Young, S. J. Dewhurst, R. M. Stevenson, P. Atkinson, A. J. Bennett, M. B. Ward, K. Cooper, D. A. Ritchie, and A. J. Shields, *New J. Phys.* **9**, 365 (2007).
- ⁵T. D. Ladd, F. Jelezko, R. Laflamme, Y. Nakamura, C. Monroe, and J. L. O'Brien, *Nature* **464**, 45 (2010).
- ⁶R. J. Warburton, *Nat. Mater.* **12**, 483 (2013).
- ⁷M. Kroutvar, Y. Ducommun, D. Heiss, M. Bichler, D. Schuh, G. Abstreiter, and J. J. Finley, *Nature* **432**, 81 (2004).
- ⁸J. R. Prance, Z. Shi, C. B. Simmons, D. E. Savage, M. G. Lagally, L. R. Schreiber, L. M. K. Vandersypen, M. Friesen, R. Joynt, S. N. Coppersmith, and M. A. Eriksson, *Phys. Rev. Lett.* **108**, 046808 (2012).
- ⁹R. Hanson, L. H. W. van Beveren, I. T. Vink, J. M. Elzerman, W. J. M. Naber, F. H. L. Koppens, L. P. Kouwenhoven, and L. M. K. Vandersypen, *Phys. Rev. Lett.* **94**, 196802 (2005).
- ¹⁰B. Marquardt, M. Geller, A. Lorke, D. Reuter, and A. D. Wieck, *Appl. Phys. Lett.* **95**, 022113 (2009).
- ¹¹B. Marquardt, M. Geller, B. Baxevanis, D. Pfannkuche, A. D. Wieck, D. Reuter, and A. Lorke, *Nat. Commun.* **2**, 209 (2011).
- ¹²B. Marquardt, A. Beckel, A. Lorke, A. D. Wieck, D. Reuter, and M. Geller, *Appl. Phys. Lett.* **99**, 223510 (2011).
- ¹³A. Beckel, A. Ludwig, A. D. Wieck, A. Lorke, and M. Geller, *Phys. Rev. B* **89**, 155430 (2014).
- ¹⁴A. Beckel, A. Kurzmann, M. Geller, A. Ludwig, A. D. Wieck, J. König, and A. Lorke, *Europhys. Lett.* **106**, 47002 (2014).
- ¹⁵R. J. Luyken, A. Lorke, A. Govorov, J. P. Kotthaus, G. Medeiros Ribeiro, and P. M. Petroff, *Appl. Phys. Lett.* **74**, 2486 (1999).
- ¹⁶To convert gate voltages V_p into energies ΔE we use the lever arm model $\Delta E = LeV_p$, where the lever arm $L = \frac{1}{2}$ is the geometric distance between the 2DEG and the quantum dot layer, divided by the geometric distance between the 2DEG and the gate.^{18,19}
- ¹⁷The value of $\tau_p = 14 \pm 2 \mu\text{s}$ was obtained from fits to the discharging characteristics [see Fig. 2(b)] for all charging times t_c .
- ¹⁸H. Drexler, D. Leonard, W. Hansen, J. P. Kotthaus, and P. M. Petroff, *Phys. Rev. Lett.* **73**, 2252 (1994).
- ¹⁹R. J. Warburton, B. T. Miller, C. S. Dürr, C. Bödefeld, K. Karrai, J. P. Kotthaus, G. Medeiros-Ribeiro, P. M. Petroff, and S. Huant, *Phys. Rev. B* **58**, 16221 (1998).
- ²⁰A. C. Johnson, J. R. Petta, J. M. Taylor, A. Yacoby, M. D. Lukin, C. M. Marcus, M. P. Hanson, and A. C. Gossard, *Nature* **435**, 925 (2005).
- ²¹S. Amasha, K. MacLean, I. P. Radu, D. M. Zumbühl, M. A. Kastner, M. P. Hanson, and A. C. Gossard, *Phys. Rev. Lett.* **100**, 046803 (2008).
- ²²H. Wei, M. Gong, G. C. Guo, and L. He, *Phys. Rev. B* **85**, 045317 (2012).
- ²³H. Wei, G. C. Guo, and L. He, *Phys. Rev. B* **89**, 245305 (2014).
- ²⁴R. Dahbashi, J. Hübner, F. Berski, K. Pierz, and M. Oestreich, *Phys. Rev. Lett.* **112**, 156601 (2014).
- ²⁵T. Fujisawa, D. G. Austing, Y. Tokura, Y. Hirayama, and S. Tarucha, *Nature* **419**, 278 (2002).
- ²⁶P. Knipp, T. Reinecke, A. Lorke, M. Fricke, and P. Petroff, *Phys. Rev. B* **56**, 1516 (1997).
- ²⁷A. V. Khaetskii and Y. V. Nazarov, *Phys. Rev. B* **61**, 12639 (2000).
- ²⁸C.-Y. Lu, Y. Zhao, A. N. Vamivakas, C. Matthiesen, S. Fält, A. Badolato, and M. Atatüre, *Phys. Rev. B* **81**, 035332 (2010).
- ²⁹F. Fras, B. Eble, P. Desfonds, F. Bernardot, C. Testelin, M. Chamarro, A. Miard, and A. Lemaître, *Phys. Rev. B* **86**, 045306 (2012).
- ³⁰F. Sotier, T. Thomay, T. Hanke, J. Korger, S. Mahapatra, A. Frey, K. Brunner, R. Bratschitsch, and A. Leitenstorfer, *Nat. Phys.* **5**, 352 (2009).
- ³¹Y. Benny, R. Presman, Y. Kodriano, E. Poem, D. Gershoni, T. A. Truong, and P. M. Petroff, *Phys. Rev. B* **89**, 035316 (2014).